Investigating the Relationship of Dampening, Length and Drop Angle on a Pendulum

Oakley Gompels
1009005871
University of Toronto
PHY324

December 21, 2025

Abstract

This experiment used measurements from a pendulum to test the theoretical predictions of damped harmonic motion by verifying period independence from amplitude, exponential decay, length scaling, and apparatus symmetry. A 50.0 ± 0.1 g cylindrical bob on a braided string was suspended from a clamp stand, with a symmetric "Y" split to ensure 2D motion and an angle setting method to remove protractor parallax. For fixed effective length $L+D$, repeated 10-cycle stopwatch timings were taken over a range of drop angles $\theta_0 \approx \pm \frac{\pi}{2}$; for fixed θ_0, the length L was varied; and a single long run at fixed (L, θ_0) was recorded and tracked to obtain the full displacement pattern. The small-angle prediction using the measured $L+D$ gave a constant period $T_0^{(\text{theory})} = 1.042 \pm 0.001$ s, and a weighted-mean constant period fit gave $T_0^{(\text{wt})} = 1.080 \pm 0.001$ s, but both models produced very large reduced chi-squared values ($\chi^2_\nu = 3430.27$ and 265.94), refuting amplitude independence. However, a power-series model $T(\theta_0) = T_0(1 + a\,\theta_0^2)$ with $T_0 = 1.030 \pm 0.002$ s and $a = 0.063 \pm 0.001$ gave $\chi^2_\nu = 1.45$ with structureless residuals, showing a quadratic increase of T with θ_0. A symmetry test fitting $T(\theta_0) = a + b\,\theta_0 + c\,\theta_0^2$ yielded $b = -0.001 \pm 0.002 \approx 0$, showing no left-right bias. Length period data fitted to $T(L) = a\,(L+D)^b$ with fixed $D = 0.045 \pm 0.001$ m gave $a = 2.030 \pm 0.006$ and $b = 0.46 \pm 0.04$ with $\chi^2_\nu = 4.69$, supporting the expected $T \propto (L+D)^{1/2}$ scaling, but indicating slightly underestimated uncertainties in T and/or L. Finally, the tracked displacement decay was described by $x(t) = X_{\max}\exp(-t/\tau)$ with $X_{\max} = 26.2 \pm 0.1$ cm, $\tau = 188.0 \pm 0.3$ s, and $\chi^2_\nu = 3.71$, showing an approximately exponential decay, with hints of underfitting. Finally, the decay constant τ was found to decrease with both increasing amplitude and increasing length, following $\tau(\theta_0) = \tau_0/(1+a\theta_0^2)$ with $\tau_0 = 189 \pm 4$ s and $a = 0.14 \pm 0.03$, and $\tau(L+D) = A(L+D)^B$ with $A = 220 \pm 4$ s$\cdot$m^{-B} and $B = -0.37 \pm 0.07$, consistent with velocity-dependent damping.

1 Introduction and Theory

A simple pendulum demonstrates small-angle oscillations and energy exchange. Theoretically, its period depends only on effective length and gravitational acceleration by acting as a simple harmonic oscillator. This experiment tests whether real pendulums with finite amplitude, air drag, and pivot friction match theoretical predictions.

The equation of motion for the angle $\theta(t)$ from the vertical is: $(L + D)\,\ddot{\theta}(t) + g\,\sin\theta(t) = 0$, where L is string length, D the bob offset, g the gravitational acceleration, and dots denote time derivatives.

For small angles, $\sin\theta \approx \theta$, this equation reduces to:

$$T_0 = 2\pi\sqrt{\frac{L+D}{g}} \approx 2\sqrt{L+D}, \tag{1}$$

for the approximation the constant 2 $s \cdot m^{-1/2}$ ($\approx \frac{2\pi}{\sqrt{g}}$) and square-root to be tested for $L^2 \gg D^2$ (in order for the bob to behave like a point mass) [1].

When the drop angle θ_0 is not small, the small angle approximation in Eq. (1) fails and the period gains a weak amplitude dependence. A series expansion of the exact period for moderate angles gives,

$$T(\theta_0) = T_0\left(1 + a\theta_0^2\right), \tag{2}$$

where T_0 is the initial period, and a is a fitted parameter (theory predicts a = 1/16; first non-linear correction that introduces the change in period, in the expansion).

Real oscillations are damped with coefficent, $\frac{2}{\tau}$, (which is the viscous drag proportional to velocity) gives: $\ddot{\theta}(t) + \frac{2}{\tau}\dot{\theta}(t) + \omega_0^2\,\theta(t) = 0$, where τ is the decay constant, $\omega_0 = \sqrt{\frac{g}{L+D}}$ is the natural angular frequency.

In the underdamped condition, the solution has the form: $\theta(t) = \theta_0 \exp\!\left(-\frac{t}{\tau}\right)\cos(\omega t + \phi_0)$, where ω is the weak damped angular frequency, ϕ_0 is initial phase angle. For small angles, the displacement envelope x(t) follows,

$$x_{\text{env}}(t) = X_{\max}\,\exp(-t/\tau), \tag{3}$$

with $X_{\max}$, initial amplitude. Measuring this gives a way to test whether decay is exponential and find τ.

In addition, there's no theory showing how τ depends on θ_0 or $(L+D)$, but physically, damping arises from air resistance and pivot friction. For moderate velocities, air drag $\propto v^2$, so higher amplitudes and longer pendulums should experience stronger damping. This suggests that τ might decrease with both parameters, to try capture this, a quadratic model, where τ_0 is as $\theta_0 \to 0$,

$$\tau(\theta_0) = \tau_0(1 + a\theta_0^2)^{-1} \tag{4}$$

Similarly, a power-law model

$$\tau(L+D) = A(L+D)^B \tag{5}$$

showing length dependence, where A is a dimensional constant and B is the scaling exponent.

This experiments aim is to test five main claims from the lab manual [1]: Period is independent of the drop angle at fixed length; Amplitude decays exponentially (find the decay constant, τ); Period is dependent on length at fixed drop angle; That asymmetry of the apparatus can be quantified; Empirically investigate the dependence of $(L+D)$ and θ_0 on time constant.

To investigate these claims, measurements were taken in three configurations: varying θ_0 at fixed L to study amplitude effects; varying L at fixed θ_0 to test the length scaling; and recording full swings with varying (L, θ_0) to extract the decay constant τ.

By the end of the experiment, comparing the fitted results with the theoretical ones from Eqs. (1)–(5) allows each of the claims to be verified or refuted.

Beyond these specific predictions, I will also investigate how the decay constant τ depends on both amplitude and length by fitting empirical functions and justifying by goodness of fit.

2 Method

2.1 Apparatus and Initial Setup

The pendulum (Fig. 7) used a 50.0 ± 0.1 g cylindrical bob on braided string suspended from a clamp stand. Early trials revealed two issues: non-planar motion from pivot friction and protractor parallax when measuring θ_0. The setup was redesigned to enforce 2-D motion and measure θ_0 geometrically. See Appendix C,Fig. (7) for a detailed diagram of the apparatus.

2.2 Design Decisions to Enforce 2-D Motion

Rather than adding damping surfaces, the braided string was split into two strands 5 cm below the pivot, forming a symmetric, Y, that kept horizontal tension components equal and opposite, suppressing twist while maintaining airflow. The centred Y was taped in place, removing precession and making left-right releases symmetric.

2.3 Angle Setting and Calibration

Protractor parallax was eliminated by using a guide wire from pivot to table as a geometric reference. Measuring horizontal and vertical distances with the tape measure (±1 mm uncertainty each) gave $\theta_0 = \arctan\left(\frac{\text{horizontal}}{\text{vertical}}\right)$, and releasing the bob parallel to the wire made angles reproducible for symmetry checks. Minimizing a large uncertainty from using a protractor, (from ±0.07 rad, down to ±0.02 rad)

2.4 Period Measurements

Periods were measured using an iPhone 14 stopwatch (±0.01 s resolution) by timing 10 cycles per run to average out reaction time. Each data point represents the mean of six 10-cycle timings (three per side), with standard error as the uncertainty. Length L was measured with a 1 meter tape measure (±1 mm uncertainty); same bob at constant D ($= 0.045 \pm 0.001$m) and $L^2 \gg D^2$.

2.5 Damping Measurements and Video Tracking

Damping was measured by recording motion until decay (30 fps video, 1x zoom) with the camera parallel (checked with built-in level) to the swing plane at bob height to minimize distortion. $1cm^2$ Blue tape on the centre of mass of bob to improve contrast for Tracker 6.1.1 analysis [2], which auto-tracked 20 frames using string length for calibration, yielding 25,600 (t,x,y) points. Peak amplitudes gave the exponential decay, with uncertainties from template-matching tolerance (±0.1 cm) propagated through peak finding.

2.6 Control of Non-Essential Variables and Uncertainty Reduction

The bob mass and orientation were fixed, the stand cleared the swing plane so the string didn't brush the rod, and releases started from rest to avoid transverse velocity. Design choices targeted symmetry (centred "Y" split), repeatability (geometric angle setting, 10-cycle timing), and uncertainty reduction (parallel camera, high contrast), making the procedure reproducible while addressing dominant error sources. (More in Appendix. B)

3 Results

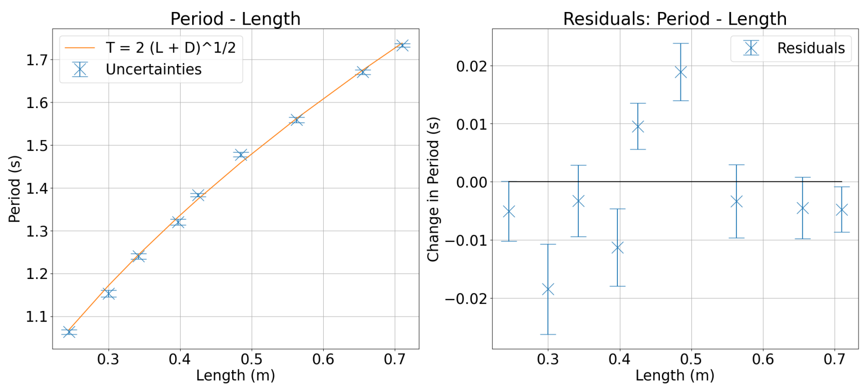

Figure 1: Period T vs length L at fixed amplitude with square-root fit, $T(L) = a\,(L + D)^b$ ($a = 2.030 \ \pm \ 0.006,\ b = 0.46 \ \pm \ 0.04,\ \chi^2_\nu = 4.69$), showing that the data approximately follows $\sqrt{L + D}$, but elevated χ^2_ν and mid-length structure suggests underfitting. Residuals reinforce this, showing an underestimation of uncertainties, since only 50% of points cross zero.

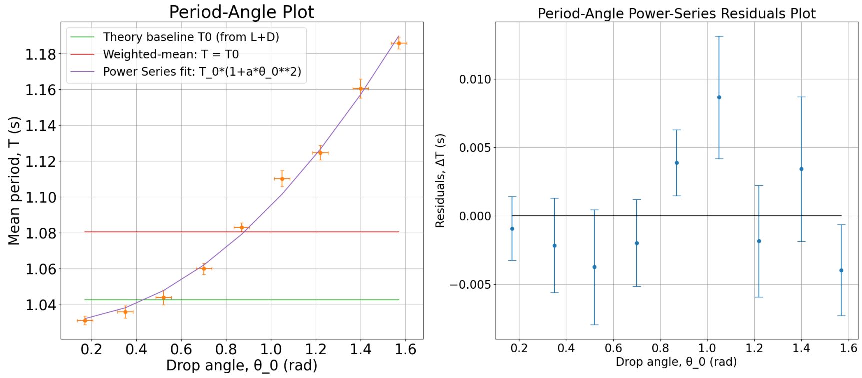

Figure 2: Mean period T vs drop angle θ_0 at fixed length. Error bars show standard error (vertical) and angle uncertainty (horizontal). Small-angle prediction from $L + D$ (green line): $T_0^{(\mathrm{th})} = 1.042 \pm 0.001$ s, $\chi^2_\nu = 3430.27$. Angle-independent weighted-mean model (red line): $T_0^{(\mathrm{wt})} = 1.080 \pm 0.001$ s, $\chi^2_\nu = 265.94$. Power-series model Eq (2): $T_0 = 1.030 \pm 0.002$ s, $a = 0.063 \pm 0.001$, $\chi^2_\nu = 1.45 \sim 1$. Power-series model residuals show a random scatter with $\chi^2_\nu = 1.45$ and 66% of the uncertainties crossing zero; this dependence on θ_0 is probable, and the uncertainties are well estimated.

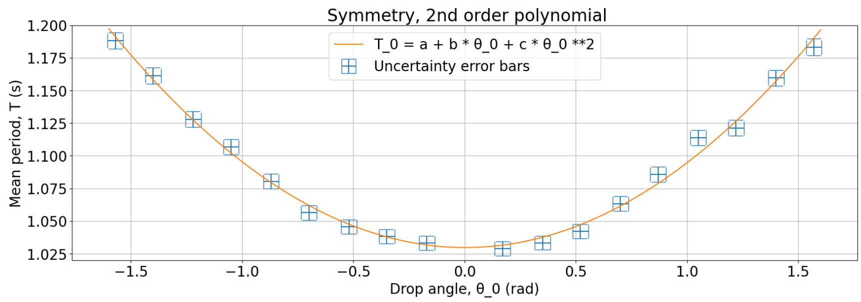

Figure 3: Mean period, $T(\theta_0)$ with polarity on the drop angles. Fitted to a 2nd order polynomial: $a = 1.030 \pm 0.004$, $b = -0.001 \pm 0.002$, and $c = 0.065 \pm 0.003$. A linear coefficient, $b \approx 0$, provides evidence of no detectable asymmetry in the apparatus. A residuals plot is unnecessary here, as $\chi^2_\nu = 1.23 \approx 1$, confirming the model describes the data without systematic deviations that would warrant further visualization.

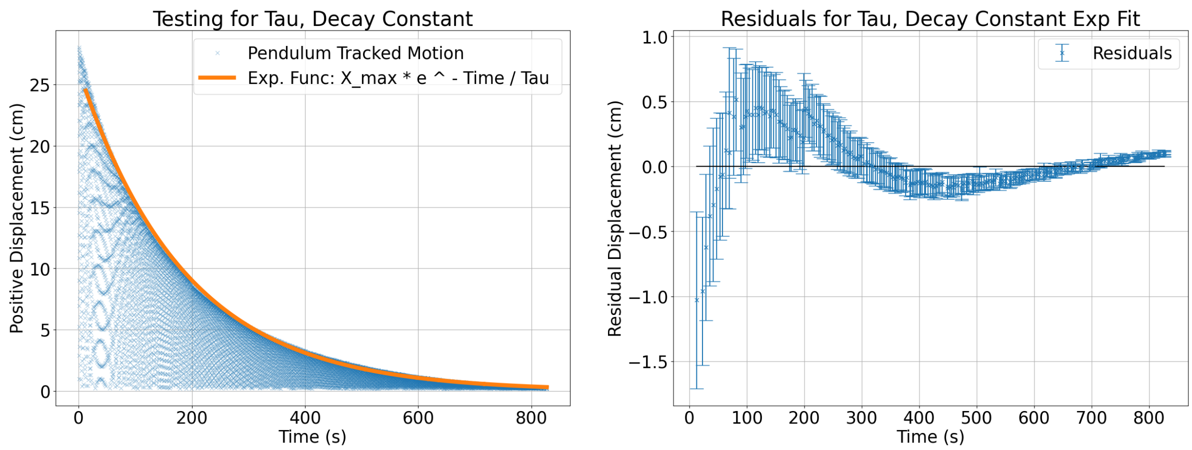

Figure 4: Positive displacement of motion fitted to an exponential (Eq. 3). From 10,000 tracked (t,x,y) points over 827 s. Fitting gives: $X_{\max} = 26.2 \pm 0.1$ cm, $\tau = 188.0 \pm 0.3\ s$, $\chi^2_\nu = 3.71$. The residuals are small relative to the overall decay but exhibit a pattern consistent with a decaying sinusoidal wave, with a reduced chi-squared value $\chi^2_\nu = 3.71$, indicating slight under-fitting, and only 33.8% of cross zero

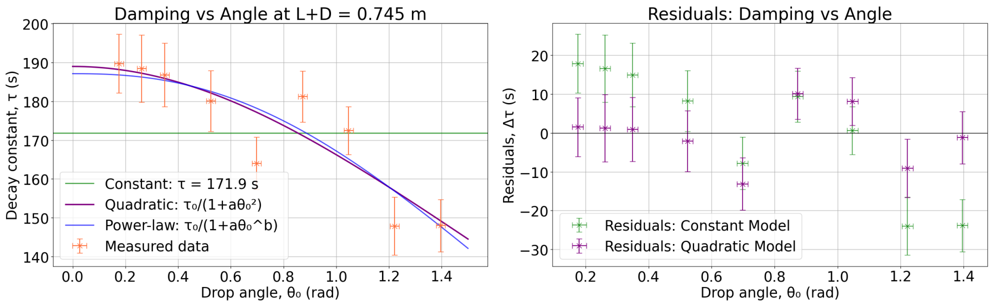

Figure 5: Mean decay constant τ as a function of drop angle θ_0 at fixed $L + D = 0.745 \pm 0.001$ m. Angle-independent weighted-mean model (green line): $\tau_{\text{const}} = 171 \pm 2$ s, $\chi^2_\nu = 4.97$, which rejects the hypothesis that damping is amplitude-independent, enforced by power law structure in residuals (green). Quadratic model (Eq. 4)(purple curve): $\tau_0 = 189 \pm 4$ s, $a = 0.14 \pm 0.03$, $\chi^2_\nu = 1.36$ and structureless residuals. Power-law model (blue dotted curve): $b = 2 \pm 1$, consistent with the quadratic form within uncertainty, so the simpler 2-parameter model is preferred.

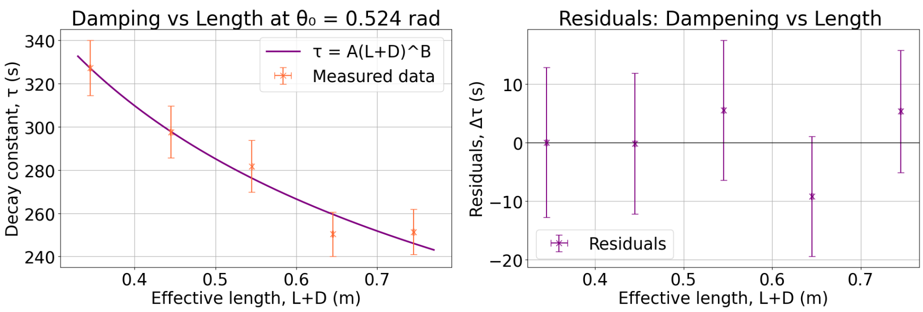

Figure 6: Mean decay constant was examined by measuring τ across five different lengths $(L + D) = 0.300$-0.700 m at fixed $\theta_0 = 0.524$ rad. The purple curve is a power-law fit, Eq.(5), with $A = 220 \pm 4$ s·m^{-B} and $B = -0.37 \pm 0.07$, yielding $\chi^2_\nu = 0.43$ with randomly scattered residuals, showing that τ decreases systematically with increasing length. The negative exponent agrees that longer lengths have stronger damping.

4 Discussion

4.1 Length dependence of the period

Figure 1 tests $T = 2\sqrt{(L + D)}$ (Eq.(1)). The fit yielded $a = 2.030 \pm 0.006$ (close to $\frac{2\pi}{\sqrt{g}} \approx 2.006$) and $b = 0.46 \pm 0.04$ (consistent with 0.5) with $\chi^2_\nu = 4.69$, supporting the scaling but suggesting slightly underestimated uncertainties.

4.2 Amplitude dependence of the period

Figure 2 tests amplitude independence. The small-angle prediction $T_0^{theory} = 1.042 \pm 0.001\ s$ (green line) yields $\chi^2_\nu = 3430.27$ with systematic curvature in residuals, strongly rejecting the constant period model as deviations exceed 1σ error bars.

A weighted-mean fit $T_0^{wt} = 1.080 \pm 0.001$ s still shows systematic curvature ($\chi^2_\nu = 265.94$) (see Appendix C, Figure 8), confirming that large χ^2_ν values reflect a model failure rather than underestimated uncertainties.

Equation (2) gave $T_0 = 1.030 \pm 0.002$ s and a $= 0.063 \pm 0.001$ ($\chi^2_\nu = 1.45$) with structureless residuals. The fit matches the theoretical prediction ($\frac{1}{16} = 0.0625$), and T increases 14% across the angle range, refuting amplitude independence while supporting the small-angle approximation for $\theta_0 < 0.3$ rad.

4.3 Quantified asymmetry of the pendulum

Figure 3 tests whether left and right releases produce identical periods by fitting $T(\theta_0) = a + b\theta_0 + c\theta_0^2$ to signed angles, yielding linear term $b = -0.001 \pm 0.002$, statistically consistent with zero. This confirms the absence of asymmetric bias, validates the centred, Y, split design, and justifies combining data from both sides to reduce uncertainty.

4.4 Exponential Decay and Decay Constant

Figure 4 tests exponential decay (Eq. (3)), yielding $X_{max} = 26.2 \pm 0.1$ cm and $\tau = 188.0 \pm 0.3$s ($\chi^2_\nu = 3.71$). The fit follows the overall decay well, consistent with exponential form despite slight underfitting. The dominant uncertainty in τ measurements arose from tracking the bob position.

The residuals show a decaying oscillatory pattern ($\chi^2_\nu = 3.71$), likely from tracking errors, non-2D motion, or breakdown of the small-angle approximation at large initial amplitudes. Non-linear damping (amplitude-dependent air drag and pivot friction) may also contribute slight deviations, though the overall exponential trend is robust.

4.5 Tau Dependence on Length and Drop Angle

Figures (5,6) show τ depends on both θ_0 and $L + D$, by evaluating the relationship using empirical fits with the goodness of fit.

The quadratic amplitude dependence (Eq. (4): $a = 0.14 \pm 0.03$) parallels the period finding (Fig. 2: $a = 0.063 \pm 0.001$). The factor of two differences is consistent with v^2 scaling drag forces affecting τ, versus restoring forces affecting period.

Length dependence $\tau \propto (L + D)^{-0.37}$ indicates air resistance dominates over pivot , likely due to the cylindrical shape of the bob. The exponent $B = -0.37 \pm 0.07 < -0.5$ in pure velocity scaling, suggesting additional factors present. Unlike the small-angle period prediction, which has a clear prediction, τ depends sensitively on amplitude and dimensions.

5 Conclusion

This experiment tested four claims of the simple pendulum model using a custom apparatus designed for symmetry, large angles, and controlled geometry. The claim that the period T is independent of amplitude was clearly refuted, both the theoretical constant period from Eq.(1) and the weighted-mean model produced extremely large reduced chi-squared values ($\chi^2_\nu = 3430.27$ and 265.94), whereas the quadratic model from Eq. (2) provided an excellent fit ($\chi^2_\nu = 1.45$) with $T_0 = 1.030 \pm 0.002$ s and $a = 0.063 \pm 0.001$, matching the expected $a_{\text{th}} = 1/16$. The symmetry test showed $b \approx 0$ in the fit to $T(\theta_0) = a + b\theta_0 + c\theta_0^2$, confirming that left right releases are statistically similar and the "Y" split enforced 2D motion.

Length-Period measurements supported $T \propto (L+D)^{1/2}$, ($a = 2.030 \pm 0.006$, $b = 0.46 \pm 0.04$, $\chi^2_\nu = 4.69$). Displacement decay followed exponential form ($X_{max} = 26.2 \pm 0.1$cm, $\tau = 188.0 \pm 0.3\ s$, $\chi^2_\nu = 3.71$) despite oscillatory residuals from tracking errors or non-linear damping.

The decay constant τ decreased with both amplitude ($\tau_0 = 189 \pm 4\ s,\ a = 0.14 \pm 0.03,\ \chi^2_\nu = 1.36$) and length ($B = -0.37 \pm 0.07,\ \chi^2_\nu = 0.43$), consistent with velocity-dependent damping where longer pendulums experience greater air resistance.

The dominant uncertainty in period measurements was reaction time ($\pm$ 0.01 s per timing / $\sqrt{60}$ measurements $\approx \pm$ 0.001 s per point). Photogate timing would reduce this to instrumental resolution ($\approx \pm 0.0001$s), improving T_0 precision by an order of magnitude. The dominant systematic uncertainty was geometric angle measurement ($\pm$ 0.02 rad from $\pm$ 1 mm horizontal/vertical positioning). A calibrated protractor with $\pm 0.5°$ precision would reduce this to $\pm$ 0.009 rad, halving the contribution to $\chi^2_\nu = 4.69$ in the length-period fit.

Overall, the experiment confirms and aligns with theory that the real pendulum: (i) exhibits a quadratic increase of period with amplitude, (ii) behaves symmetrically for left and right releases, (iii) follows the expected $T \propto (L + D)^{1/2}$ scaling with length, and (iv) decays approximately exponentially with $\tau \approx 188$ s, (v) Tau is dependent on both $(L + D)$ and θ_0.

6 Appendix

References

[1] Department of Physics, *PHY324 Pendulum Project - 2025*, University of Toronto, 2025.

[2] Open Source Physics, *Tracker Online - 2025*, opensourcephysics.github.io/tracker-online.

A Collaboration and Use of AI

Collaboration: I, Oakley Gompels, conducted the data, carried out the analysis and wrote the report. The experiment was conducted in tandem with Isabella Schick, due to a lack of equipment and space, but the data was collected separately and analysis was done independently, under the supervision of the instructor.

Use of AI: Parts of this LaTeX report were revised with assistance from an AI tool (ChatGPT) to improve grammar, clarity, and logical flow. Any AI-generated text has been reviewed and validated by the author for accuracy and completeness.

B Uncertainty budget and dominant error sources

Across all parts of the experiment, the dominant *Type A* (statistical) uncertainties arise from the spread of repeated 10-cycle timings and from the scatter in Tracker related positions error from not being the same point on the bob each time. These are represented by the standard errors of the mean in Figs. 2-1 and by the grouping uncertainties in Figs. 4. Because these error bars are relatively small, the reduced chi-squared values provide a sensitive test of the models.

The main *Type B* (systematic) sources are: (i) geometric calibration of the drop angle θ_0 from horizontal and vertical; (ii) length measurement with the tape (± 1 mm) and distance of attachment point to centre of mass, D; and (iii) camera calibration/parallax into Tracker (pixel to length scaling and frame rate). For the amplitude study, these Type B effects mostly shift all periods up or down by a small amount and slightly rescale θ_0, but they cannot mimic the strong quadratic trend that drives the failure of the constant-period models. For the length dependence and damping measurements, the elevated χ^2_ν values and the residual patterns could suggest that the calculated statistical errors underestimate the true uncertainties.

In summary, Type A uncertainties control the visible scatter in the plots, while Type B uncertainties are the likely causes of the moderate differences between the fitted parameters and the proposed theoretical constants (e.g. $a \approx 2$ and $b \approx 0.5$).

C Additional Plots and Figures

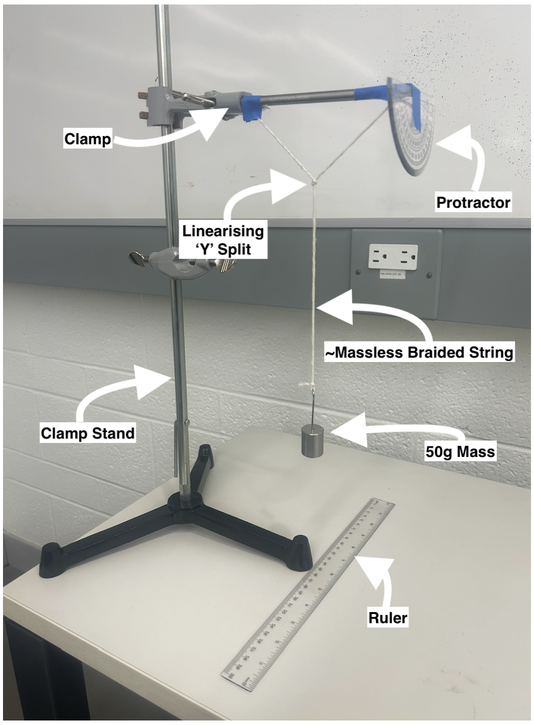

Figure 7: Pendulum apparatus: A 50 g cylindrical bob is suspended by a braided string that is split into a symmetric "Y" $\approx$ 5 cm below the pivot to suppress twist and enforce planar (2-D) motion. The string is hung from a clamp mounted on a rigid stand; a protractor is shown for initial alignment only (final angle setting was done geometrically, as described in the text). A ruler provides scale and was used to measure the length L from the pivot to the bob's attachment point; the stand is positioned so the string clears the rod to avoid contact-induced asymmetry.

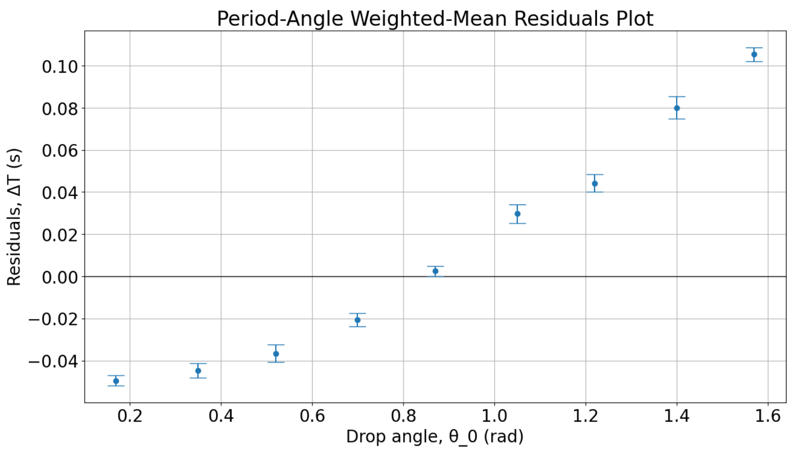

Figure 8: Residuals ΔT between the measured mean period and the angle-independent weighted-mean model. The strong systematic curvature with θ_0 and the large reduced chi-squared $\chi^2_\nu = 265.94$ demonstrate that a constant-period model is improbable with the data.